Supporting Information for

Many-Body Polarization Effects and the Membrane Dipole Potential

Edward Harder,[†]

Alexander D. MacKerell Jr.[*‡] and Benoit Roux[*†]

[†]Department of Biochemistry and Molecular Biology, Center for Integrative Science, University of Chicago, Chicago, Illinois, 60637

[‡]Department of Pharmaceutical Sciences School of Pharmacy University of Maryland Baltimore, Maryland, 21201

[*] Corresponding authors e-mail: roux@uchicago.edu alex@outerbanks.umaryland.edu

1. COMPUTATIONAL DETAILS

Initial configurations for monolayer-air and water-air simulations are constructed from pre-equilibrated configurations of a hydrated lipid bilayer and bulk water, respectively. The bilayer system consists of 72 DPPC molecules and 2825 water molecules. The bulk water system consists of 500 molecules. The final configuration of the bilayer has the unit cell dimensions 47.6 x 47.6 x 76.2 Å and is used to build an air-monolayer-monolayer-air system by translating the bilayer leaflets and extending the unit cell along the membrane normal to 150 Å. The bulk water system is extended along a unit cell dimension from 24.8 Å to 75 Å to create an air-water-air system. Both the monolayer-air and water-air simulations are performed in the NVT ensemble at a temperature of 320 K under 3D periodic boundary conditions with the electrostatic forces evaluated using a particle mesh approximation to the Ewald sum.[1]

All molecular dynamics simulations were performed with the program CHARMM[2] using a velocity Verlet algorithm.[3] The temperature is controlled by a Nosé-Hoover thermostat.[4] The SHAKE/Roll and RATTLE/Roll procedure[5,6] are used to constrain covalent bonds to hydrogens. A smooth real space cutoff is applied between 10-12 Å an Ewald splitting parameter of 0.34 $Å^{-1}$ a grid spacing of $\approx$ 1.0 Å and a 6th order interpolation of the charge to the grid is used. The same cutoff scheme is used for the Lennard-Jones potential and a long range correction to the energy and pressure from the LJ potential is included.[3]

The electrostatic degrees of freedom are minimized at the outset of the simulation and propagated dynamically along with the nuclei. For appropriately chosen kinetic variables so-called extended Lagrangian simulations provide an accurate and efficient alternative to a self-consistent field solution at each time step of the simulation.[7,8] A mass of 0.1 amu is added to the free end of the Drude oscillator and subtracted from the reference heavy atom. The equations of motion are integrated with a 1 fs time step for the polarizable model and a 2 fs time step for the nonpolarizable model. Both the monolayer-air and water-air systems are equilibrated for 1 ns and statistics are averaged over 5 ns. Data is further averaged over the pair of interface regions.

QM calculations of the molecular dipole for the 27 rotamers of the esterified glycerol molecule was performed using the QCHEM program.[9]

2. THE MONOLAYER DIPOLE POTENTIAL

The observable under investigation is the difference between a potential measured between the water and air phases of a bare water-air interface and the potential measured between the same phases upon adsorption of a lipid monolayer. To draw quantitative comparison between simulation and experiment it is important to consider possible contributions that may not be accounted for in the model. One such consideration is the salt concentration present in experiment[10] but not in the simulations. However, this effect has been shown to provide a negligible impact on the monolayer potential in a similar regime (salt concentration + phosphatidylcholine lipids) to that under investigation.[11]

---

[1] Essmann, U.; Perera, L.; Berkowitz, M. L.; Darden, T.; Lee, H.; Pedersen, L. G. *J. Chem. Phys.* **1995**, *103*, 8577.

[2] MacKerell, Jr., A. D.; Brooks, B.; Brooks, III, C. L.; Nilsson, L.; Roux, B.; Won, Y.; Karplus, M. *CHARMM: The Energy Function and Its Parameterization with an Overview of the Program. In Encyclopedia of Computational Chemistry*, Vol. 1; John Wiley & Sons,Chichester, 1998.

[3] Allen, M. P.; Tildesley, D. J. *Computer Simulation of Liquids;* Oxford University Press Inc., New York, 1987.

[4] Martyna, G. J.; Klein, M. L.; Tuckerman, M. *J. Chem. Phys.* **1992**, *97*, 2635–2643.

[5] Martyna, G. J.; Tuckerman, M. E.; Tobias, D. J.; Klein, M. L. *Mol. Phys.* **1996**, *87*, 1117–1157.

[6] Andersen, H. C. *J. Comput. Phys* **1983**, *52*, 24.

[7] Harder, E.; Kim, B.; Friesner, R. A.; Berne, B. J. *J. Chem. Theory and Comput.* **2005**, *1*, 169.

[8] Lamoureux, G.; Roux, B. *J. Chem. Phys.* **2003**, *119*, 3025–3039.

[9] Shao, Y.; Fusti-Molnar, L.; Jung, Y.; Kussmann, J.; Ochsenfeld, C.; Brown, S. T.; Gilbert, A. T.; Slipchenko, L. V.; Levchenko, S. V.; O'Neill, D. P.; DiStasio Jr., R. A.; Lochan, R. C.; Wang, T.; Beran, G. J. O.; Besley, N. A.; Herbert, J. M.; Lin, C. Y.; Voorhis, T. V.; Chien, S. H.; Sodt, A.; Steele, R. P.; Rassolov, V. A.; Maslen, P. E.; Korambath, P. P.; Adamson, R. D.; Austin, B.; Baker, J.; Byrd, E. F. C.; Daschel, H.; Doerksen, R. J.; Dreuw, A.; Dunietz, B. D.; Dutoi, A. D.; Furlani, T. R.; Gwaltney, S. R.; Heyden, A.; Hirata, S.; Hsu, C.-P.; Kedziora, G.; Khalliulin, R. Z.; Klunzinger, P.; Lee, A. M.; Lee, M. S.; Liang, W.; Lotan, I.; Nair, N.;

Peters, B.; Proynov, E. I.; Pieniazek, P. A.; Rhee, Y. M.; Ritchie, J.; Rosta, E.; Sherrill, C. D.; Simmonett, A. C.; Subotnik, J. E.; Woodcock, III, H. L.; Zhang, W.; Bell, A. T.; Chakraborty, A. K.; Chipman, D. M.; Keil, F. J.; Warshel, A.; Hehre, W. J.; Schaefer, III, H. F.; Kong, J.; Krylov, A. I.; Gill, P. M.; Head-Gordon, M. *Phys. Chem. Chem. Phys* **in press**.

[10] Smaby, J. M.; Brockman, H. L. *Biophys. J.* **1990**, *58*, 195–204.

[11] Mingins, J.; Stigter, D.; Dill, K. A. *Biophys. J.* **1992**, *61*, 1603–1615.

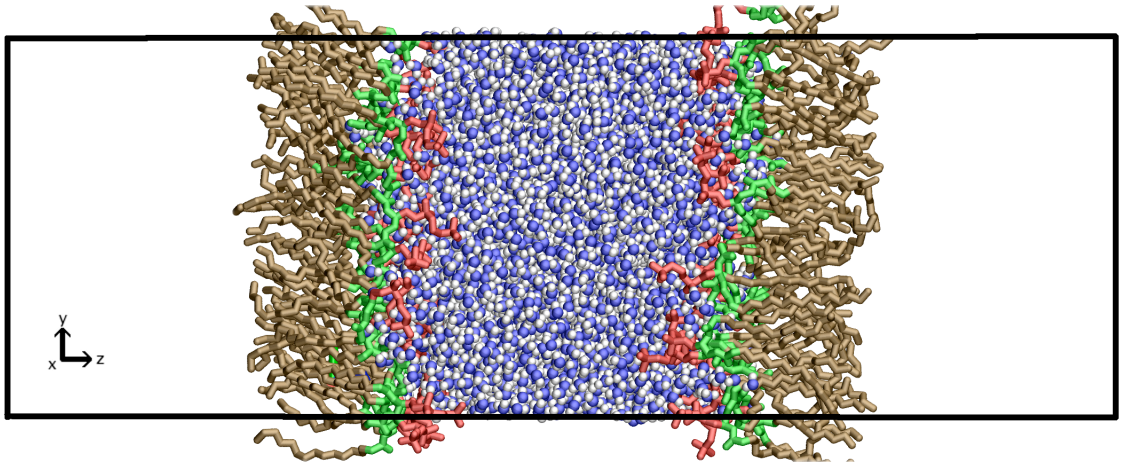

FIG. 1: A coordinate snapshot from the simulation of the adsorbed monolayer on a water-air interface. Indicated in the figure is the simulation unit cell. Colors are in accord with the designation of molecule types in Figure 1 of the manuscript. Blue corresponds to water, red atoms are part of the PC head group, green atoms correspond to the ester moeity and brown atoms correspond to the hydrocarbon tails of the lipid molecules.

TABLE I: The component breakdown to the membrane dipole potential of a monolayer at a water-air interface. The POL and NONPOL models correspond to the polarizable Drude and nonpolarizable CHARMM models, respectively.

Potential	Pol	NonPol
V_{water}	4.2	2.6
V_{PC}	-2.9	-2.4
V_{ester}	-0.1	0.7
$V_{\text{aliphatic}}$	-0.3	0.4
$V_{\text{mono-air}}$	0.9	1.3
ΔV	0.35	0.8

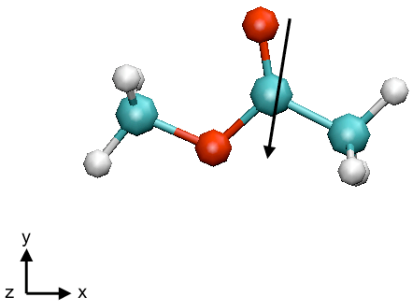

FIG. 2: Orientation of methyl acetate used to characterize the gas phase electrostatic properties. The arrow represents the direction of the molecular dipole from a QM calculation at the B3LYP/aug-cc-pVDZ level.

TABLE II: The methyl acetate dipole. The model lies in the x,y plane with the principal geometric axis aligned with the Cartesian x-axis. The QM model is computed at the B3LYP/aug-cc-pvdz level. The Pol and NonPol models correspond to the polarizable Drude and nonpolarizable CHARMM models, respectively. The nonpolarizable ESTERμ model is parameterized to reproduce the gas phase electrostatic properties of the ester moiety.

Potential	Exp.	QM	POL	NONPOL	ESTERμ
μ_x		0.3	0.2	-1.3	0.4
μ_y		1.9	1.7	2.1	1.8
μ_z		0.0	0.0	0.0	0.0
μ	1.7	1.9	1.7	2.3	1.8

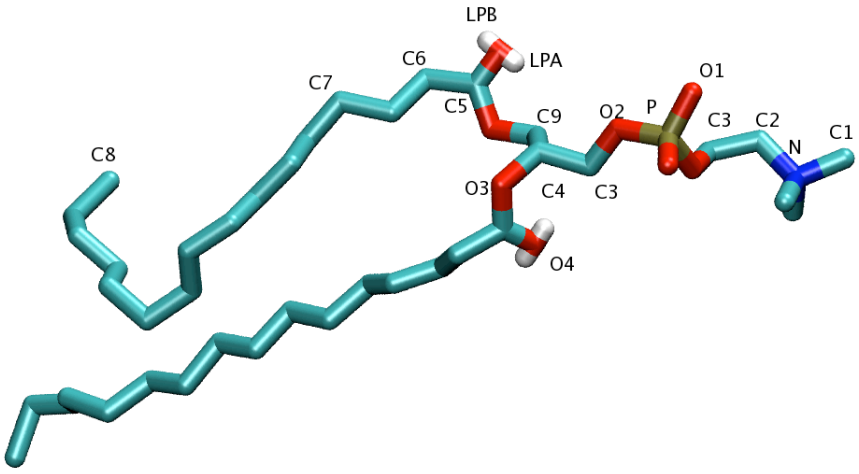

FIG. 3: Atom type labels for Pol model parameters

TABLE III: Pol model parameters.

atom type	q (e)	α (Å^3)	$R_{min}/2$ (Å)	ϵ (kcal/mol)
N	0.688	-0.829	1.74	-0.2
C1	-0.288	-1.793	2.04	-0.078
H1	0.122	0.0	0.925	-0.046
C2	-0.166	-1.393	2.01	-0.056
C3	-0.011	-0.704	2.01	-0.056
H3	0.081	0.0	1.34	-0.035
P	1.202	-1.638	1.9	-0.46
O1	-0.816	-1.126	1.91	-0.13
O2	-0.436	-1.257	1.76	-0.14
C4	0.206	-0.997	1.74	-0.078
H4	0.119	0.0	1.34	-0.035
O3	-0.365	-0.732	1.755	-0.1521
C5	0.696	-1.370	2.0	-0.07
O4	-0.028	-0.904	1.96	-0.145
C6	-0.194	-1.593	1.74	-0.078
H6	0.070	0.0	1.34	-0.035
LP-A	-0.322	0.0	0.0	0.0
LP-B	-0.252	0.0	0.0	0.0
C9	0.087	-1.397	1.74	-0.078
H9	0.070	0.0	1.34	-0.035
C7	-0.156	-1.660	2.01	-0.056
H7	0.078	0.0	1.34	-0.035
C8	-0.177	-2.051	2.04	-0.078
H8	0.059	0.0	1.34	-0.024